

ENCIT-2018-0533

EFFECTS OF SOLUBILITY ON KICK DETECTION AND PRESSURE TRANSMISSION

Jonathan F. Galdino
Gabriel M. de Oliveira
Admilson T. Franco
Cezar O. R. Negrão

Research Center for Rheology and Non-Newtonian Fluids (CERNN)

Federal University of Technology - Paraná, Deputado Heitor Alencar Furtado, n° 5000, Curitiba, Brazil, 81280-340

jonathang@alunos.utfpr.edu.br, gabrielm@utfpr.edu.br, admilson@utfpr.edu.br, negrao@utfpr.edu.br

Abstract. Blowout is the most dangerous situation during well drilling operations and it only occurs when the kick, the phase that precedes a blowout, is not detected and controlled properly. Early kick detection is crucial for rig safety and is usually performed by observing the pit gain. Gas solubility reduces the pit gain. Kick control initiates by shutting-in the well and waiting for pressure stabilization. The closing pressures (SICP and SIDPP) measured at surface are used to determine the pore pressure. However, drilling fluid yield stress reduces the pressures measured. Consequently, the pore pressure and the necessary density of the drilling fluid to cease the influx may be underestimated. The purpose of this work is to develop a mathematical and numerical model to investigate the effects of gas solubility on kick detection and on pressure transmission after the well closure. The flow is assumed as transient, one-dimensional, laminar and compressible. Bingham model is employed to represent the drilling fluid behavior. Empirical correlations are used for gas solubility. The method of characteristics is employed to solve the balance equations of mass and momentum. The results indicate that gas solubility reduces considerably the pit gain and that the pressure transmission must be taken into account for a proper estimative of the pore pressure.

Keywords: kick detection, pressure transmission, yield stress, solubility, method of characteristics

1. INTRODUCTION

Decades ago, the prevailing vision among researchers was the depletion of oil reserves in the USA in few years (Packard, 1960). By the end of the 20th century, the reserves of petroleum were about ten times higher than at 1950, despite the growth of oil usage (Sowell, 2014). The same trend is true for Brazil, with the discovery of the Pre-salt area, and for Africa. These new fields of petroleum are located at great depths, requiring a higher precision during well drilling operation, once the increase of water depth reduces the operating window (Vallero and Letcher, 2012). The operating window is the range of pressure wherein the pressure must be kept during the drilling. The maximum pressure is the fracture pressure, exceeding this limit may result in the mechanical failure of the well. The minimum pressure is the pore pressure. In case the pressure falls below this inferior limit, the formation fluid (water, oil or gas) may migrate into the well (Carlsen et al., 2013). This influx is denominated as kick and the gas influx is the most dangerous due to the gas expansibility and its solubilization in non-water based drilling fluids. Therefore, kicks must be detected as soon as possible.

The most reliable kick indicator is the pit gain, which is the volume gained in the mud tanks (Islam et al., 2017). However, the high gas solubility in non-aqueous drilling fluids reduces the pit gain, making the kick detection harder (O'Bryan et al., 1988; Thomas, 2004; Ma et al., 2018). Early kick detection is crucial for the well control operation (Fraser et al., 2014; Brakel et al., 2015; Fu et al., 2015), once it reduces the closing pressures and the amount of formation fluid within the well (Fu et al., 2015). After the kick detection, the usual procedure is to shut-in the well and wait for the pressure stabilization (Nandan and Imtiaz, 2016). The closing pressures, Shut-In Drill Pipe Pressure (SIDPP) and Shut-In Casing Pressure (SICP), are constantly monitored. The SIDPP is assumed as the difference between the pore pressure and the hydrostatic pressure in the drill pipe (Bourgoyne et al., 1986). By knowing the pore pressure, the density of the drilling fluid necessary so that the hydrostatic pressure exceeds the pore pressure is calculated. However, the yield stress of the drilling fluid causes the non-total pressure transmission along the well (de Oliveira et al., 2013; Mitishita, 2015). Thereby, the pore pressure is underestimated as well as the new density of the drilling fluid to kill the kick. The likely aftermath is the continuation of the gas influx, increasing the non-productive time and putting at risk the rig safety.

Although kick detection has been well investigated, blowouts are still taking place, such as the blowout Macondo in the

USA with 11 people killed and the Kaixian blowout in China with 243 deaths. We investigate the effects of gas solubility on pit gain. Moreover, the non-total pressure transmission caused by the drilling fluid yield stress in well operations has received little attention in the academy, if any. Perhaps one of the reasons is that, in the past, the operating window was not that narrow, and the safety margin added in the increase of density of the drilling fluid compensated the effects of the yield stress. However, in narrow operating window an oversized density will cause the mechanical failure of the well. For these reasons, in order to improve the kick detection and the precision of the pore pressure estimative, this work proposes a mathematical and numerical model to predict the effects of gas solubility on the behavior of kick detection parameters as well as on the pressure transmission after the well closure. The transient model is based on the balance equations for the mixture and the non-Newtonian behavior of the drilling fluid is taken into account by the Bingham model. Furthermore, gas solubility in synthetic-based drilling fluid is considered. The results obtained by the proposed model can improve the kick detection and the calculations for the necessary density to terminate kicks, reducing the risks of the control operation and decreasing the non-productive time.

2. MATHEMATICAL MODELING

In well drilling process, the drilling fluid is pumped at the drill pipe surface, passing through the bit and returning by the annular space. The geometry adopted comprises the drill pipe and the annular space, which are concentric, as can be seen in Fig. 1. Although the well has several changes in its sections, such characteristic is disregarded in the model. It is also neglected any deformation in the well dimensions as well the presence of bit. The influx takes place at the bottom of the well and migrates only through the annular space. The initial condition is the fluid being pumped with a constant volumetric flow rate along the well without any presence of gas. The boundary conditions are: constant volumetric flow rate at the drill pipe surface and atmospheric pressure at the annular surface. The kick begins at $t = 0$ s and when the pit gain reaches a predefined value, the kick is detected, the pumps are switched off and the well is closed, changing the boundary conditions for zero volumetric flow rate at both surfaces. The simulation proceeds until the total pressure stabilization along the well.

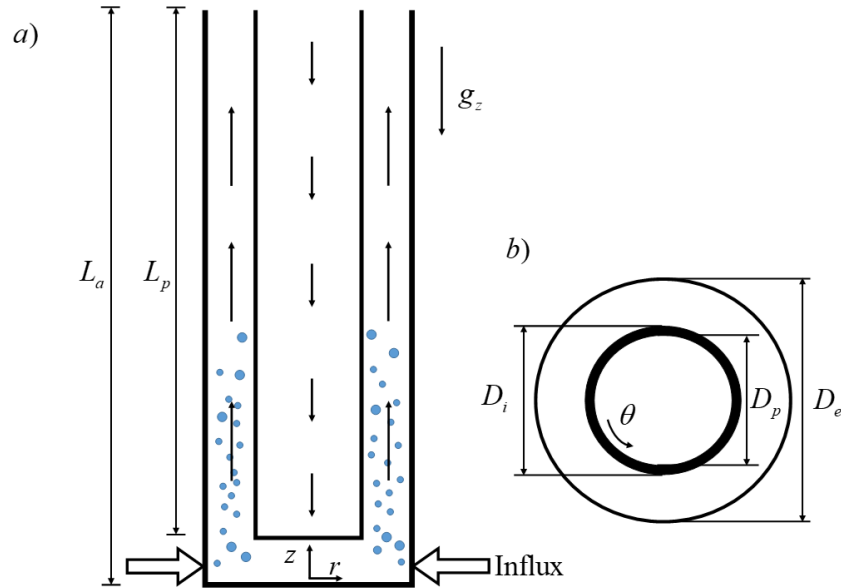


Figure 1. a) Schematic representation of the geometry and b) cross sectional of drill pipe and annular space

2.1 Governing equations

The model is based on balance equations of mass and momentum for the mixture. The two-phase flow is assumed as homogeneous, isothermal, weakly compressible and one-dimensional. Applying those assumptions, the final forms of the balance equations of mass and momentum are, respectively (Wylie *et al.*, 1993):

$$\frac{\partial P}{\partial t} + \rho_m c_m^2 \frac{\partial V}{\partial z} = 0 \quad (1)$$

$$\frac{\partial V}{\partial t} + \frac{1}{\rho_m} \frac{\partial P}{\partial z} + \frac{2fV|V|}{D_h} + g_z = 0 \quad (2)$$

where P is the pressure, t is the time, V is the velocity, z is the axial direction, ρ_m is the mixture density, c_m is the pressure-wave speed in the mixture, D_h is the hydraulic diameter, g_z is the acceleration of gravity, and f is the Fanning friction factor.

The pressure-wave speed in the mixture and mixture density for a homogeneous flow can be written as (Hage and Ter Avest, 1994; Wylie *et al.*, 1993):

$$c_m = \sqrt{\frac{\rho_l c_l^2}{[1 + \alpha(\frac{\rho_l c_l^2}{P})] \rho_m}} \quad (3)$$

$$\rho_m = \rho_l(1 - \alpha) + \rho_g \alpha \quad (4)$$

where ρ_l is the density of the liquid phase, ρ_g is the gas density, c_l is the pressure-wave speed in the liquid phase, and α is the volumetric gas void fraction.

The liquid density is assumed constant along the axial direction. However, the gas dissolution changes the liquid density. In order to take this effect into account, the empirical correlations for the oil formation volume factor, B_0 , and solubility ratio, R_s , presented by Kim (2010) are employed in this work.

Gas density is calculated employing the compressibility factor Z proposed by Yarborough and Hall (1974):

$$\rho_g = \frac{P}{ZRT} \quad (5)$$

where R is the universal gas constant.

According to Fontenot and Clark (1974), the Fanning friction factor for a Bingham fluid can be expressed as:

$$f = \frac{16\zeta}{\psi Re_{z,t}} \quad (6)$$

where ζ is a geometric factor, $Re_{z,t}$ is the Reynolds number for the mixture, and ψ is the Bingham fluid conductance.

Gas influx into the well is modeled by the Darcy's law (Dake, 1998):

$$q_g = \frac{2\pi k_r h_r (P_p - P_{BH})}{\mu_g \ln\left(\frac{r_r}{r_e}\right)} \quad (7)$$

where q_g is the radial volumetric flow rate of gas at the bottom of the well, k_r is the porous media permeability, h_r is the reservoir height, r_r is the reservoir radius, r_e is the external radius of the annular space, P_p is the pore pressure, and P_{BH} is the bottom hole pressure.

2.2 Initial and boundary conditions

The initial condition is the drilling fluid being pumped with a constant flow rate at the drill pipe surface and atmospheric pressure at the annular surface. At $t = 0$ s the drill bit reaches a reservoir with pore pressure higher than the bottom hole pressure and the gas influx takes place. The drilling fluid constant flow rate as well as the atmospheric pressure continue as boundary conditions until the kick detection. Kick is detected when a predefined pit gain is exceeded. At this moment, the pumps are switched off and the well is closed. Therefore, both boundary conditions at surface are changed to zero flow rate. The simulation continues until the pressure stabilization.

3. NUMERICAL SOLUTION

The balance equations of mass and momentum, Eqs. (1) and (2), form a pair of hyperbolic partial differential equations which do not have a known analytical solution. In order to solve the equations, the method of characteristics is applied. The method consists in transforming the hyperbolic partial differential equations into total differential equations by making a linear combination between them, resulting in two pairs of equations (Wylie *et al.*, 1993; Chaudhry, 2014):

$$C^+ : \begin{cases} \frac{1}{\rho_m c_m} \frac{dP}{dt} + \frac{dV}{dt} + \frac{2fV|V|}{D_h} - g_z = 0 & (a) \\ \frac{dz}{dt} = +c_m & (b) \end{cases} \quad (8)$$

$$C^- : \begin{cases} \frac{-1}{\rho_m c_m} \frac{dP}{dt} + \frac{dV}{dt} + \frac{2fV|V|}{D_h} - g_z = 0 & \text{(a)} \\ \frac{dz}{dt} = -c_m & \text{(b)} \end{cases} \quad (9)$$

Equations (8a) and (9a) are denominated as the compatibility equations, whereas the Eqs. (8b) and (9b) are the characteristic lines. The characteristic lines represent the change in position of a wave related to the change in time by the pressure-wave speed. Note that the spatial independent variable z was eliminated in the compatibility equations, which are only valid over the characteristic lines (Chaudhry, 2014).

The grid of the method of characteristics is shown in Fig. 2. The uniform grid has an even number of cells with length equal to $\Delta z = L_T/N$, where L_T is the total length of the domain and N is the number of cells. The time-step is a function of the pressure-wave speed in the liquid, $\Delta t = \Delta z/c_l$. The black dashed lines represent the pressure-wave speed in the liquid over time and space. Once this velocity is constant, the lines are straight. However, as aforementioned, the presence of free gas decreases the pressure-wave speed. Therefore, the lines are no longer straight and the grid becomes non-uniform. Moreover, the characteristic lines that cross the point i do not come from the points $i-1$ and $i+1$, but instead they come from the points R and S . In order to maintain a uniform grid and a fixed time-step, it is performed a linear interpolation to determine the properties values at the points R and S and the predictor-corrector technique is applied (Wylie *et al.*, 1993). By integrating the compatibility equations over the characteristic lines, velocity and pressure at next time-step, $n+1$, can be determined.

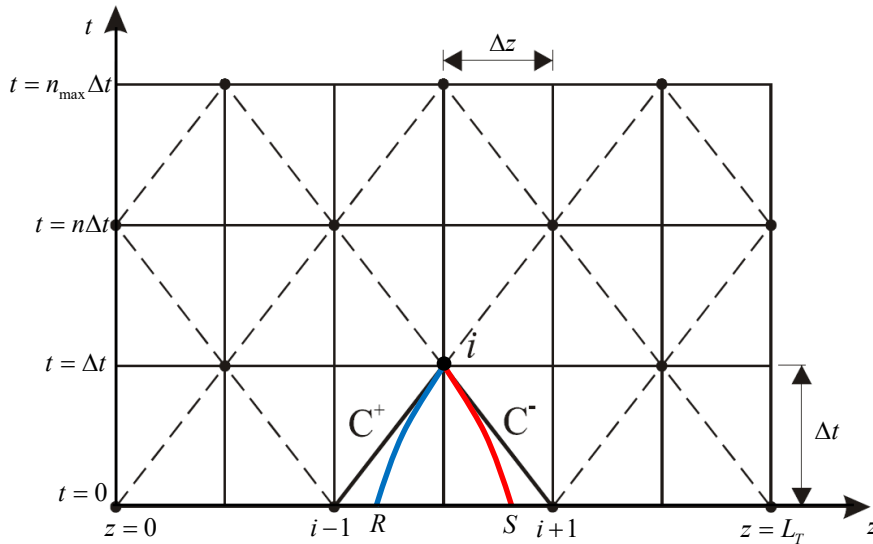


Figure 2. Grid of the method of characteristics.

4. RESULTS

In this section we presented two kick simulations with two different types of drilling fluid in order to investigate the effects of gas solubility on kick detection and pressure transmission. One drilling fluid is water-based and the other is synthetic-based. Since gas solubility is very small in water-based muds, it is neglected in this case. The parameters employed in the simulations are shown in Tab. 1.

First we analyze the effect of gas solubility on pit gain. Pit gain is the level increase in the mud pits and it is the most employed kick indicator (Anfinsen and Rommetveit, 1992; Mitchell and Miska, 2011; Ali *et al.*, 2013). As aforementioned, pit gain with non-aqueous fluids are considerable smaller than the pit gain with WBMs (O'Bryan *et al.*, 1988; An *et al.*, 2015; Ma *et al.*, 2018). The pit gain over time for the two different drilling fluid types is presented in Fig. 3. With the synthetic-based drilling fluid, when gas enters the well, all gas comes in solution, occupying a small volume. Therefore, there is a small increase in the pit gain. When using the water-based mud, gas enters as free gas, displacing a higher volume of the drilling fluid toward surface, resulting in a higher pit gain. At $t = 600$ s, the pit gain in SBM is less than half of the pit gain in WBM. Moreover, with the SBM, kick detection took more than 1200 s whereas it took about half the time with WBM.

Table 1. Parameters employed in the simulations.

| | | | |
|----------------|--|-------------------------|----------------------|
| Geometry | Well length | 4,000 | m |
| | Drill pipe diameter | 0.127 | m |
| | Internal diameter of the annular space | 0.139 | m |
| | External diameter of the annular space | 0.216 | m |
| Drilling fluid | Density | 981 | kg/m ³ |
| | Pressure-wave speed | 1000 | m/s |
| | Plastic viscosity | 0.1 | Pa.s |
| | Yield stress | 8.0 | Pa |
| | Ester volumetric fraction | 70% | - |
| | Pump flow rate | 0.03 | m ³ /s |
| Gas influx | Pit gain limit for detection | 0.318 | m ³ |
| | ΔP to the reservoir | 0.5 | MPa |
| | Darcy's constant | 5.465×10^{-10} | m ⁴ .s/kg |
| | Gas constant (methane) | 518.3 | J/kg.K |
| | Gas temperature | 323 | K |
| Simulation | Cell length | 8 | m |
| | Time-step | 8 | ms |

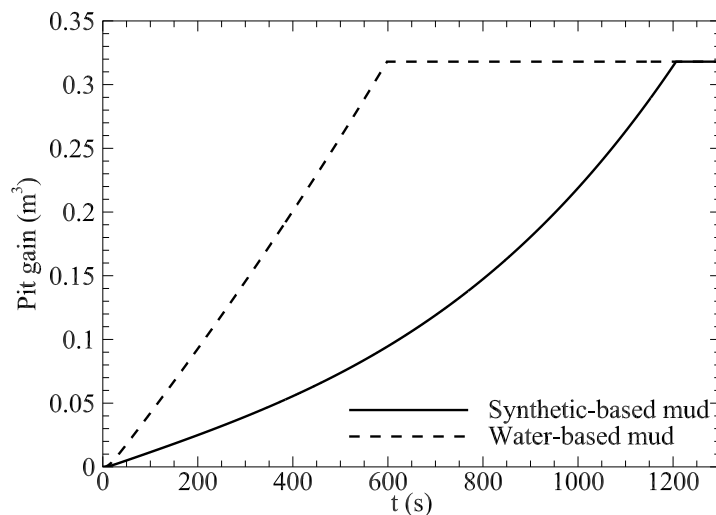


Figure 3. Pit gain for SBM and WBM.

Now it is performed a study case comparing the real pore pressure with the value that would be calculated using the conventional procedure in the oil industry, which considers a total pressure transmission. The purpose is to emphasize the effects of the drilling fluid yield stress on the well control operation. Figure 4 presents the pressure profile (discounting the hydrostatic pressure) along the drill pipe and annular space when the pressures are stabilized at $t = 3000$ s. In the oil industry, the closing pressures are assumed to represent the difference between the pore pressure and the hydrostatic pressure (Mitchell and Miska, 2011). If the drilling fluid were Newtonian, the pressure profile represented in Fig. 4 would be constant along the well length. However, that is not the case with real drilling fluids due to the yield stress. The curve inclination represents the degree of pressure attenuation. Note that the pressure profile in the drill pipe is independent of the drilling fluid type and that there is a pressure attenuation of 1.07 MPa. By using the conventional formulas, the estimated pore pressure would be 45.16 MPa whereas, in reality, the real pore pressure is 46.23 MPa. By the conventional calculation, it would be necessary a drilling fluid density of 1152 kg/m³. But in fact, the real necessary density is 1178 kg/m³. According to Skalle (2011), it is usually added a safety margin of 50 kg/m³. By adding the safety margin, in this

case, the kick would be successfully ceased. However, in other cases the operating window may be so narrow that this safety margin cannot be added and the influx would continue in the next stop. Moreover, SICP is higher with water-based mud because the decrease in hydrostatic pressure was higher with this fluid. The higher the hydrostatic pressure drop, the greater the annular closing pressure.

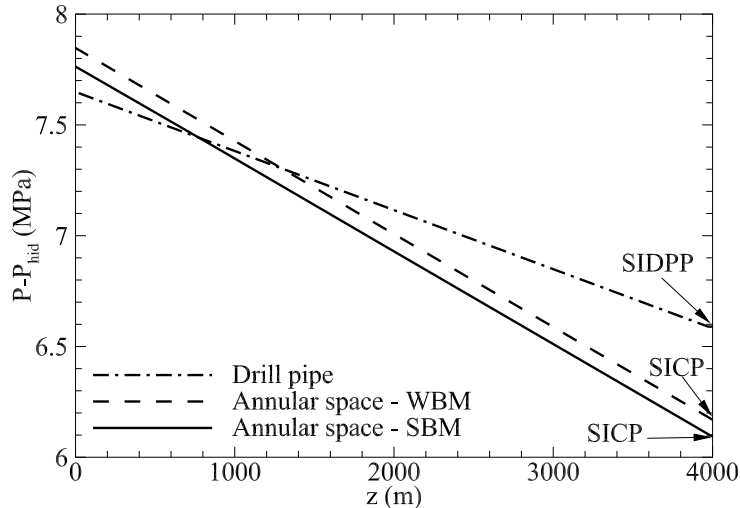


Figure 4. Pressure transmission along the well for SBM and WBM.

5. CONCLUSION

In this work we presented a transient mathematical and numerical model to predict effects of solubility on pit gain and on the pressure transmission after the well closure. The model, based on the balance equation of mass and momentum for the mixture, comprises the compressibility and the non-Newtonian behavior of the drilling fluid. Moreover, gas solubility in synthetic drilling fluids is taken into account. In summary, the results indicate that:

- Gas kick in non-aqueous drilling fluids takes considerably more time to be detected;
- The shut-in casing pressure in non-aqueous drilling fluids is higher than in water-based drilling fluid for a same pit gain;
- The final value of the shut-in drill pipe pressure is not affected by gas solubility;
- Pressure attenuation caused by drilling fluid yield stress plays an important role in the estimative of the pore pressure and must be taken into account for a proper well control procedure.

6. ACKNOWLEDGEMENTS

The authors acknowledge the financial support of PETROBRAS S/A, ANP (Brazilian National Oil Agency) and CNPq (The Brazilian National Council for Scientific and Technological Development).

7. REFERENCES

- Ali, T.H., Haberer, S.M., Says, I.P., Ubaru, C.C., Laing, M.L., Helgesen, O., Liang, M., Bjelland, B. *et al.*, 2013. “Automated alarms for smart flowback fingerprinting and early kick detection”. In *SPE/IADC Drilling Conference*. Society of Petroleum Engineers.
- An, J., Lee, K., Choe, J. *et al.*, 2015. “Well control simulation model of oil-based muds for hpht wells”. In *SPE/IATMI Asia Pacific Oil & Gas Conference and Exhibition*. Society of Petroleum Engineers.
- Anfinson, B. and Rommetveit, R., 1992. “Sensitivity of early kick detection parameters in full-scale gas kick experiments with oil-and water-based drilling muds”. In *SPE/IADC Drilling Conference*. Society of Petroleum Engineers.
- Bourgoyne, A.T., Millheim, K.K., Chenevert, M.E. and Young, F.S., 1986. *Applied drilling engineering*. Society of Petroleum Engineers Richardson.
- Brakel, J., Tarr, B., Cox, W., Jorgensen, F., Straume, H.V. *et al.*, 2015. “Smart kick detection: First step on the well-control automation journey”. *SPE Drilling & Completion*, Vol. 30, No. 03, pp. 233–242.

- Chagas, F.L.d.S., 2016. *Estudo da operação de controle de poços com fluidos de perfuração sintéticos*. M.S.thesis, University of Campinas.
- Chaudhry, M.H., 2014. *Applied hydraulic transients*. Springer.
- Dake, L.P., 1998. *Fundamentals of Reservoir Engineering*, Vol. 8. Elsevier Science.
- de Oliveira, G.M., Franco, A.T., Negrão, C.O., Martins, A.L. and Silva, R.A., 2013. "Modeling and validation of pressure propagation in drilling fluids pumped into a closed well". *Journal of Petroleum Science and Engineering*, Vol. 103, pp. 61–71.
- Fontenot, J.E. and Clark, R., 1974. "An improved method for calculating swab and surge pressures and circulating pressures in a drilling well". *Society of Petroleum Engineers Journal*, Vol. 14, No. 05, pp. 451–462.
- Fraser, D., Lindley, R., Moore, D. and Vander Staak, M., 2014. "Early kick detection methods and technologies". In *SPE Annual Technical Conference and Exhibition*. Society of Petroleum Engineers.
- Fu, J., Su, Y., Jiang, W. and Xu, L., 2015. "Development and testing of kick detection system at mud line in deepwater drilling". *Journal of Petroleum Science and Engineering*, Vol. 135, pp. 452–460.
- Hage, J. and Ter Avest, D., 1994. "Borehole acoustics applied to kick detection". *Journal of Petroleum Science and Engineering*, Vol. 12, No. 2, pp. 157–166.
- Hauge, E., 2013. "Automatic kick detection and handling in managed pressure drilling systems".
- Islam, R., Khan, F. and Venkatesan, R., 2017. "Real time risk analysis of kick detection: Testing and validation". *Reliability Engineering & System Safety*, Vol. 161, pp. 25–37.
- Kim, N.R., 2010. *Estudo do comportamento PVT de misturas de metano e fluidos de perfuração base éster*. Ph.D. dissertation, University of Campinas.
- Ma, Z., Vajargah, A.K., Chen, D., van Oort, E., May, R., MacPherson, J., Becker, G., Curry, D. *et al.*, 2018. "Gas kicks in non-aqueous drilling fluids: A well control challenge". In *IADC/SPE Drilling Conference and Exhibition*. Society of Petroleum Engineers.
- Meng, Y., Xu, C., Wei, N., Li, G., Li, H. and Duan, M., 2015. "Numerical simulation and experiment of the annular pressure variation caused by gas kick/injection in wells". *Journal of Natural Gas Science and Engineering*, Vol. 22, pp. 646–655.
- Mitchell, R. and Miska, S.Z., 2011. *Fundamentals of Drilling Engineering*. SPE textbook series. Society of Petroleum Engineers. ISBN 9781555632076.
- Mitishita, R.S., 2015. *Avaliação experimental da transmissão de pressão em tubulações preenchidas por fluidos viscoplásticos*. M.S.thesis, Federal University of Technology - Paraná.
- Nandan, A. and Imtiaz, S., 2016. "Nonlinear model predictive controller for kick attenuation in managed pressure drilling". *IFAC-PapersOnLine*, Vol. 49, No. 7, pp. 248–253.
- Nayeem, A.A., Venkatesan, R. and Khan, F., 2016. "Monitoring of down-hole parameters for early kick detection". *Journal of Loss Prevention in the Process Industries*, Vol. 40, pp. 43–54.
- O'Bryan, P.L., Bourgoyne Jr, A.T., Monger, T.G., Kocpcso, D.P. *et al.*, 1988. "An experimental study of gas solubility in oil-based drilling fluids". *SPE Drilling Engineering*, Vol. 3, No. 01, pp. 33–42.
- Packard, V., 1960. *The Waste Makers*. David McKay.
- Skalle, P., 2011. *Pressure control during oil well drilling*. BookBoon.
- Sowell, T., 2014. *Basic Economics: A Common Sense Guide to the Economy*. Basic Books.
- Thomas, J.E., 2004. *Fundamentos da Engenharia do Petróleo*. Interciência.
- Torsvik, A., Skogestad, J.O., Linga, H. *et al.*, 2017. "An experimental study of gas influx in oil-based drilling fluids for improved modelling of high-pressure, high-temperature wells". *SPE Drilling & Completion*.
- Wylie, E.B., Streeter, V.L. and Suo, L., 1993. *Fluid transients in systems*, Vol. 1. Prentice Hall Englewood Cliffs, NJ.
- Yarborough, L. and Hall, K.R., 1974. "How to solve equation of state for z-factors?" *Oil & Gas J*, Vol. 72, pp. 86–88.

8. RESPONSIBILITY NOTICE

The authors are the only responsible for the printed material included in this paper.